Received: 26 March 2021 | Revised: 22 July 2022 | Accepted: 25 July 2022

DOI: 10.1111/mmi.14967

RESEARCH ARTICLE

WILEY

Listeria monocytogenes two component system PieRS regulates secretion chaperones PrsA1 and PrsA2 and enhances bacterial translocation across the intestine

Laty A. Cahoon[1] | Xiomarie Alejandro-Navarreto[1] | Avinash N. Gururaja[1] | Sam H. Light[2] | Francis Alonzo[3] | Wayne F. Anderson[4] | Nancy E. Freitag[1]

[1]Department of Microbiology and Immunology, University of Illinois at Chicago, Chicago, Illinois, USA

[2]Department of Microbiology, University of Chicago, Chicago, Illinois, USA

[3]Department of Microbiology and Immunology, Loyola University, Chicago, Illinois, USA

[4]Center for Genomics and Infectious Diseases, Feinberg School of Medicine, Northwestern University, Chicago, Illinois, USA

Correspondence
Nancy E. Freitag, Department of Microbiology and Immunology, University of Illinois at Chicago, Chicago, IL, USA.
Email: nfreitag@uic.edu

Funding information
National Institute of Allergy and Infectious Diseases, Grant/Award Number: AI083241 and AI115954

Abstract

Listeria monocytogenes (*Lm*) is a widespread environmental Gram-positive bacterium that can transition into a pathogen following ingestion by a susceptible host. To cross host barriers and establish infection, *Lm* is dependent upon the regulated secretion and activity of many proteins including PrsA2, a peptidyl-prolyl *cis-trans* isomerase with foldase activity. PrsA2 contributes to the stability and activity of a number of secreted virulence factors that are required for *Lm* invasion, replication, and cell-to-cell spread within the infected host. In contrast, a second related secretion chaperone, PrsA1, has thus far no identified contributions to *Lm* pathogenesis. Here we describe the characterization of a two-component signal transduction system PieRS that regulates the expression of a regulon that includes the secretion chaperones PrsA1 and PrsA2. PieRS regulated gene products are required for bacterial resistance to ethanol exposure and are important for bacterial survival during transit through the gastrointestinal tract. PrsA1 was also found to make a unique contribution to *Lm* survival in the GI tract, revealing for the first time a non-overlapping requirement for both secretion chaperones PrsA1 and PrsA2 during the process of intra-gastric infection.

KEYWORDS
chaperone, *listeria*, PPIase, PrsA1, PrsA2, secretion

1 | INTRODUCTION

Virulence factor secretion is a fundamental aspect of bacterial pathogenesis. In Gram-positive bacteria secreted proteins are translocated in an unfolded state to enter the space that exists between the membrane and cell wall (Sarvas et al., 2004; van Wely et al., 2001). This space is solvent exposed, has a characteristically high cation concentration, and high density of negative charge that presents a challenging environment for protein folding and function (Sarvas et al., 2004). The presence of dedicated secretion chaperones are likely required to maintain optimal secretion homeostasis necessary for protein folding, activity, and correct localization. Chaperones that function to promote bacterial secretion may be required in greater quantities during conditions leading to increased protein secretion such as during host infection and/or under high stress conditions that promote protein denaturation and aggregation.

Lm is a Gram-positive bacterium that is ubiquitous in the environment but is capable of transitioning into an intracellular pathogen upon the consumption of contaminated food by the human host (Freitag et al., 2009). In the United States, *Lm* has caused numerous

multi-state food-borne outbreaks which have resulted in thousands of illnesses and hundreds of deaths with immunocompromised populations being the most at risk, including the elderly, pregnant women and neonates (Hernandez-Milian & Payeras-Cifre, 2014; Lomonaco et al., 2015; Lund, 2015). The bacterium's transition from life in the outside environment to life within the cytosol of host cells is accompanied by the increased expression and elaboration of a number of secreted virulence factors that facilitate survival by promoting cell entry, bacterial escape from host vacuoles, replication within the cytosol, and spread to adjacent cells (Alonzo & Freitag, 2010; de las Heras et al., 2011; Mostowy & Cossart, 2012; Mueller & Freitag, 2005; Port & Freitag, 2007; Shetron-Rama et al., 2003). The transcriptional activator PrfA regulates the expression of many of these secreted virulence factors required for bacterial survival within the host (Freitag et al., 1992; Leimeister-Wachter et al., 1990; Mengaud et al., 1991).

Lm has two PrsA homologs: PrsA1 and PrsA2 that are members of the parvulin peptidyl-prolyl isomerase (PPIase) family that catalyze the *cis-trans* isomerization of peptide bonds N-terminal to proline residues in polypeptide chains (Alonzo et al., 2011). PrsA1 and PrsA2 are lipid modified and membrane-associated but a significant amount of each is also secreted (Alonzo et al., 2009; Cahoon & Freitag, 2015). *Lm* mutants lacking PrsA2 exhibit decreased hemolytic and phospholipase activity, are defective for cell-to-cell spread, and are significantly less virulent in mice (Alonzo et al., 2009; Cahoon et al., 2016; Cahoon & Freitag, 2015; Forster et al., 2011; Zemansky et al., 2009). In contrast, while PrsA1 shares 75% amino acid similarity and 58% identity with PrsA2, it makes no detectable contribution in *Lm* pathogenesis-associated activities or in mouse intravenous infection models suggesting that the protein may have evolved a more general physiological chaperone function (Alonzo et al., 2009; Cahoon et al., 2016). Bacteria lacking *prsA2* also exhibit defects associated with a number of physiological activities including swimming motility, growth at acidic and basic pH and growth at high osmolarity (Alonzo et al., 2011; Cahoon et al., 2016; Cahoon & Freitag, 2015; Forster et al., 2011) while once again in contrast, mutants lacking *prsA1* have no detectable phenotype for these activities. However, *prsA1* mutants are more susceptible to cell wall active antibiotics but this sensitivity is only apparent when *prsA2* is also completely absent (Cahoon et al., 2016). Although *prsA1* thus far appears to play a minor role in *Lm* physiology, the allele is well conserved within *Lm* strains suggesting that selective pressure exists to maintain this gene.

The expression of *prsA2* is directly regulated by the transcriptional activator PrfA and increased levels of PrsA2 are necessary to maintain bacterial viability under conditions where PrfA is activated and multiple virulence-associated gene products are secreted (Ahmed & Freitag, 2016; Alonzo & Freitag, 2010). However, deletion of the PrfA binding site within the *prsA2* promoter does not significantly influence bacterial survival within the host (Zemansky et al., 2009), an observation that strongly suggests that additional mechanisms exist to increase *prsA2* expression. Additional regulatory mechanisms would likewise be consistent with the requirement for PrsA2 activity for flagella-mediated swimming motility, an activity that is negatively regulated following PrfA activation (Cahoon & Freitag, 2015). However, other mechanisms that serve to regulate *prsA2* expression as well as mechanisms underlying the regulation of *prsA1* expression have thus far not been described. Here we describe the fortuitous identification and subsequent characterization of a novel two-component system (TCS) PieRS that regulates *prsA1*and *prsA2* as well as additional gene products. Analysis of PieRS and its associated regulon reveals a requirement for PieRS during intragastric infection as well as unique non-overlapping roles for PrsA1 and PrsA2 that contribute to translocation of *Lm* across the intestinal barrier.

2 | RESULTS

2.1 | Identification of a second site suppressor mutation that partially compensates for the loss of PrsA2 chaperone activity

As part of our original identification and characterization of *prsA2* and its encoded gene product, we sought to generate a *Lm* strain containing a chromosomal in-frame deletion of *prsA2* (Alonzo et al., 2009). However, repeated attempts to generate this mutant using the standard approach of allelic exchange by homologous recombination proved unsuccessful (Alonzo et al., 2009). The construction of in-frame deletions in target genes in *Lm* requires several cycles of bacterial dilution and outgrowth in broth culture, and mutations that confer even subtle growth defects can reduce fitness such that wild type cells out-compete the mutant and take over the culture. We therefore undertook the construction of a *prsA2* mutant using Targetron insertions that could be targeted specifically to *prsA2* (Alonzo et al., 2009). Once the *prsA2* Targetron mutant (*prsA2::T*) was successfully generated, we used this mutant strain as a starting point for the generation of a *prsA2* deletion mutant containing an erythromycin resistance gene (*erm*) inserted in place of the *prsA2* coding sequences; this erythromycin-linked *prsA2* mutation could then be transferred by phage transduction into a clean wild type genetic background as well as into additional *Lm* strains.

Characterization and comparison of the original *prsA2::T* mutant with *prsA2::erm* transductants revealed immediately apparent phenotypic differences. Whereas the original *prsA2::T* mutant exhibited normal swimming motility as well as levels of secreted hemolytic and phospholipase activity that were comparable to wild type strains, the *prsA2::erm* mutant transductants (Δ*prsA2*) exhibited defects in swimming motility and reduced secreted listeriolysin O (LLO) activity and secreted phospholipase (PC-PLC) activity (Figure 1a–c). The Δ*prsA2::erm* mutant phenotypes were consistently observed for independently generated transductants and could be complemented by the introduction of *prsA2* on a plasmid chromosomal integration vector (Alonzo et al., 2009), indicating that the mutant phenotypes were linked to Δ*prsA2::erm*. While the Targetron-generated *prsA2*::T mutant exhibited normal swimming motility and hemolytic and

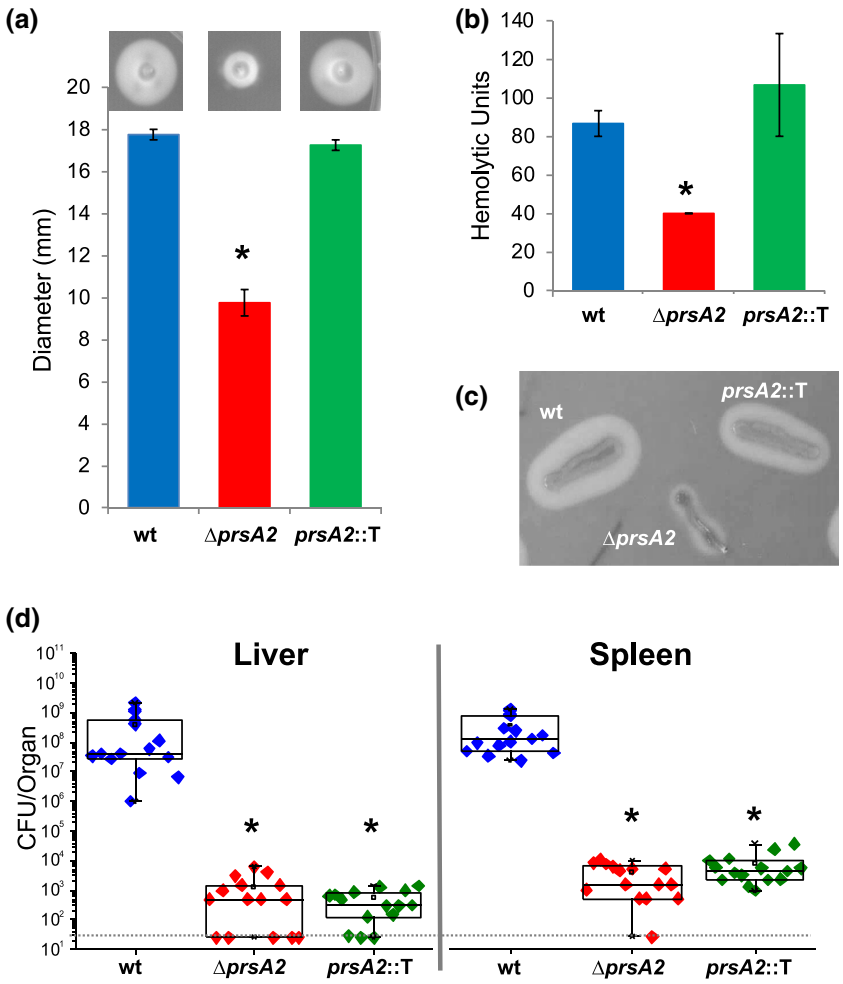

FIGURE 1 Phenotypic characterization and comparison of Δ*prsA2* and the second site suppressor mutant, *prsA2*::T. (a) Swimming motility. The diameter of the wild type (WT), *prsA2* mutant (Δ*prsA2*), and *prsA2* Targetron suppressor mutant (*prsA2*::T) swimming colonies was measured and is expressed as the average of 4 independent experiments. Error bars represent the standard error of the mean where $p \leq .05$ by two-tailed Student's T-test when compared to WT as indicated by an asterisks. (b) Hemolytic activity. The ability of bacterial culture supernatants to lyse sheep red blood cells (RBC) was assessed. The reciprocal of the supernatant dilution that resulted in 50% RBC lysis (hemolytic units) was determined. Error bars represent the standard error of the mean for 3 independent experiments where $p \leq .05$ by two-tailed Student's T-test when compared to WT as indicated by an asterisks. (c) Phospholipase activity. Strains were incubated on *listeria* selective agar plates containing lecithin that when hydrolyzed produces a zone of opacity surrounding the bacterial streak, a representative is shown for three independent experiments. (d) Mouse bacterial burdens. Mice were intravenously infected with 2×10^4 colony forming units (CFUs) with the indicated strains. At 72 h post-infection bacterial burdens were determined for livers and spleens. Box plots are shown where each point represents one animal ($N = 15$). A dotted line indicates the limit of detection. Asterisks indicate statistical significance of $p \leq .05$, by two-tailed Wilcoxon rank-sum test when compared to WT.

phospholipase activity in the absence of *prsA2* complementation, it remained highly attenuated in mouse intravenous infection models (Figure 1d). These data strongly suggested that the *prsA2::T* mutant contained a second site suppressor mutation that partially compensated for the loss of PrsA2 activity but did not restore virulence.

2.2 | Identification of PieRS and its associated gene regulon

Whole genome sequencing analysis of *prsA2*::T was performed to identify the second site suppressor mutation that partially restored PrsA2 activity. A mutation resulting in the substitution of a valine for a glutamate at position 81 (E81V) in the gene product encoded by *lmo1507* was identified within the *prsA2::T* genome (Figures S1a and 2a). Lmo1507 is predicted to function as the response regulator of a two-component signal transduction system (TCS) for which Lmo1508 is the predicted sensor histidine kinase (Figure 2a). The TCS *lmo1507-1508* is flanked by *lmo1509*, encoding a putative exodeoxyribonuclease and *lmo1505-1506* encoding a putative ABC transporter ATP-binding protein and a putative macrolide ABC transporter permease, respectively (Figure 2a).

In silico analysis suggests the response regulator Lmo1507 consists of a receiver domain with a predicted phosphorylation site

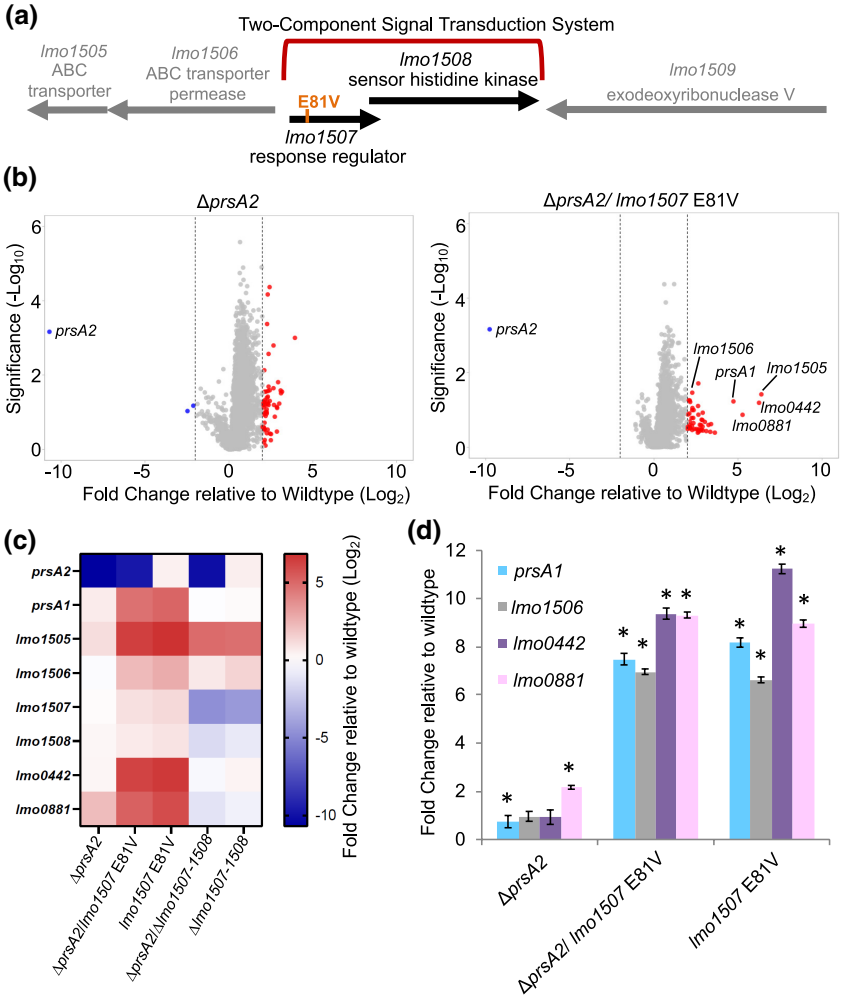

FIGURE 2 Identification of the *lmo1507-1508* (*pieRS*) operon. (a) Schematic representation of the location of the *prsA2* suppressor mutation. Whole genome sequencing of the Δ*prsA2* suppressor mutant revealed a nucleotide substitution in *pieR* resulting in E81V substitution. PieR is part of a putative two component regulatory system where PieR is the response regulator and PieR is the sensor histidine kinase. The *pieR/pieS* is flanked by *lmo1509*, encoding a putative exodeoxyribonuclease V, and *lmo1505/lmo1506*, encoding a putative ABC transporter ATP-binding protein and putative ABC transporter permease. (b) Microarray analysis. Volcano plots display the fold change comparison of the *prsA2* deletion mutant (Δ*prsA2*, left) and the the *prsA2* suppressor mutant (Δ*prsA2/pieR* E81V, right) compared to wildtype. Each symbol represents one gene in the *Lm* genome. A dotted line indicates a fold change of 2 and −2. (c) Heat map. Gene expression level relative to wildtype are indicated, genes predicted to be regulated by the PieR/PieS regulon are shown. (d) Quantitative real time PCR analysis. Expression of predicted PieR regulated genes was determined by qRT-PCR of the Δ*prsA2*, Δ*prsA2/pieR* E81V, and *pieR* E81V strains as compared to wildtype levels (WT). Genes identified by microarray analysis were upregulated in the Δ*prsA2/pieR* E81V and *pieR* E81V strains. Error bars represent the standard error of the mean where $p \leq .05$ by two-tailed Student's T-test when compared to WT as indicated by an asterisk.

at aspartic acid position 51, in addition to a DNA binding domain (Figure S1a,b) (Lu et al., 2020; Mistry et al., 2021). The Lmo1507 receiver domain also contains glutamic acid and aspartic acid at positions 7 and 8, respectively predicted to be important for metal ion-dependent phosphorelay reactions, and threonine at position 78 predicted to interact with the phosphoryl group of phosphorylated D51 (Figure S1a,b) (Lu et al., 2020). Two additional residues in the receiver domain, tyrosine and lysine at positions 97 and 100 respectively, are predicted to be important for phosphorylation mediated conformational changes (Figure S1a,b) (Lu et al., 2020). The Lmo1507 E81V mutation resides in the receiver domain between the predicted phosphorylation site D51 and residue Y97 important for phosphorylation mediated conformational changes (Figure S1a,b). A structural prediction of Lmo1507 indicates that E81 is in proximity to Y97 (Figure S1b) (Kelley et al., 2015).

In order to identify genes whose expression could potentially be regulated by the Lmo1507-1508 TCS, we constructed *Lm* mutants containing the *lmo1507* E81V mutation or deletion of *lmo1507-1508* in the presence and absence of *prsA2* and compared patterns of bacterial gene expression to the wild-type strain. DNA microarray analysis disregarding fold change differences indicates that 1144 genes are significantly different from wild-type in the Δ*prsA2* mutant which is reduced to 259 genes in the Δ*prsA2 lmo1507* E81V strain (the Δ*prsA2* suppressor mutant) (Figure S2a). Disregarding fold

change differences, the *lmo1507* E81V mutant has 559 genes significantly different than wild-type, whereas the Δ *lmo1507-lmo1508* strain and the Δ*prsA2* Δ *lmo1507-lmo1508* have comparable levels of genes significantly different than wildtype, 228 and 227, respectively (Figure S2a).

Volcano plot analysis shows that four genes are highly upregulated at over 4-fold Log_2 in the Δ*prsA2* suppressor mutant but not in the *ΔprsA2* strain (Figure 2b). These genes: *lmo1505*, *lmo0442*, *lmo0881*, and *prsA1* are also similarly upregulated in the *lmo1507* E81V mutant (Figures 2b and S2b). In addition, *lmo1506* between *lmo1505* and *lmo1507* was modestly upregulated at over 2-fold Log_2 in strains containing the *lmo1507* E81V mutation (Figures 2b and S2b). In the absence of the Lmo1507-1508 TCS, *lmo1505* remained upregulated regardless of the presence or absence of *prsA2* (Figure S2c,d). A heat map of the relative expression levels of the *lmo1507-1508* encoded TCS and putative regulon shows that strains containing the *prsA2* suppressor mutation have similar expression patterns which are distinct from strains that are deleted for the TCS (Figure 2c). We used qRT-PCR analysis to confirm the microarray data indicating increased expression of putative Lmo1507 regulated genes (Figure 2d), suggesting that the E81V mutation serves to activate Lmo1507. The function of the *lmo0881* gene product is unknown, whereas *lmo0442* encodes a fructose-specific phosphotransferase transport system (PTS) component permease that has been implicated in virulence (Liu et al., 2017) while *prsA1* encodes a peptidyl-prolyl *cis-trans* isomerase molecular chaperone that shares 75% similarity and 58% identity to PrsA2 (Alonzo et al., 2009). As mentioned previously, *lmo1507-1506* are predicted to encode a putative ABC transporter ATP-binding protein and a putative macrolide ABC transporter permease, respectively. Based on the critical requirement for PrsA1 and PrsA2 for bacterial survival under a variety of stress conditions (Cahoon et al., 2016; Cahoon & Freitag, 2015) and the ability of Lmo1507-1508 to induce the expression of *prsA1* and *prsA2*, we have designated Lmo1507-1508 as PieRS, for PrsA induced expression system component R and S.

2.3 | Characterization of the PieR response regulator

A protein BLAST search of PieRS revealed that the TCS is orthologous to the YclJ/YclK TCS of *Bacillus subtilis*. PieR is 71% identical and 82% similar to *B. subtilis* response regulator YclJ (Figure 3a), while PieS is 47% identical and 67% similar to *B. subtilis* histidine kinase YclK. Over-expression of the *B. subtilis* YclJ response regulator in a Δ*yclK* sensor kinase strain was used together with microarray analysis to associate YclJ with the regulation of several genes (Kobayashi et al., 2001) of which two (*yclH* and *yclI*) encode gene products that are homologous with two of those predicted for the PieRS TCS regulon. *B. subtilis* YclH/YclI are an ABC transporter ATP-binding protein and a putative macrolide ABC transporter permease, respectively, that share similarity with Lmo1505-1506; the genes encoding YclH and YclI are also similarly located adjacent to the TCS genes (Figure S3).

In *B. subtilis*, the DNA binding site of YclJ has been determined (Ogura et al., 2010); in silico analysis of the YclJ binding site sequence in *Lm* indicated putative binding sites consisting of the consensus sequence TTCAT-AG-TTTGT-TCATATTTN upstream of all genes in the TCS PieRS regulon (Figure 3b). Putative binding sites located 88 base pairs upstream of *prsA1*, 75 base pairs upstream of *lmo1505-1506*, 57 base pairs upstream of *lmo0442*, and 54 base pairs upstream of *lmo0881* were identified based on the YclJ DNA binding consensus sequence. The *prsA2* gene has two potential DNA binding sites located 105 base pairs and 469 base pairs upstream of *prsA2* coding sequences. Following further in silico analysis using a BLAST search (Altschul et al., 1990), one additional putative PieR binding site was identified 52 base pairs upstream of *htrA* which encodes a serine protease/chaperone. However, this appears to be a degenerate PieR binding site with a thymine at position 6 instead of an adenine which may explain why *htrA* was not identified by microarray analysis.

To test whether PieR and PieR E81V (hereafter referred to as PieR*, based on the apparent activation of the mutant protein) bound to DNA containing the putative DNA binding consensus sequence present within the upstream regions of target genes of the PieRS regulon, we performed electrophoretic mobility shift assays (EMSA). Purified N-terminal His-tagged PieR or PieR* was incubated with target DNA containing either the *prsA1* or *prsA2* putative PieR binding sites (Figure 3c,d). PieR and PieR* both bound the *prsA1* putative consensus binding site with PieR* observed to bind with an apparent higher affinity based on signal intensity (Figure 3c,d). Binding was specific as PieR* binding was reduced in the presence of unlabeled *prsA1* upstream competitor DNA, and PieR* remained bound to the labeled DNA in the presence of non-specific competitor DNA (Figure 3d). The region upstream of *prsA2* contains two putative PieR binding sites located 105 base pairs (site B) and 469 base pairs (site A) upstream of the *prsA2* ATG start site (Figure 3b). The *prsA2* sites A and B are unique when compared to the other putative PieR binding sites in that they are located further upstream from the translation initiation codon and each contains base pair insertions that differ from the consensus sequence (Figure 3b). EMSA analysis of these two sites demonstrated that PieR * had a slightly higher binding affinity for the region upstream of *prsA2* containing site B when compared to the region containing site A (Figure 3e). These data suggest that the expression of both post-translocation secretion chaperones PrsA1 and PrsA2 are directly regulated by the TCS PieRS.

2.4 | The PieR E81V (PieR*) mutation confers partial suppression for the loss of PrsA2 activity via upregulation of *prsA1*

Given that (1) PrsA1 is a molecular chaperone of the same family as PrsA2, and (2) its expression was up-regulated in the Δ*prsA2* strain containing the PieR E81V (PieR*) gain of function mutation, we postulated

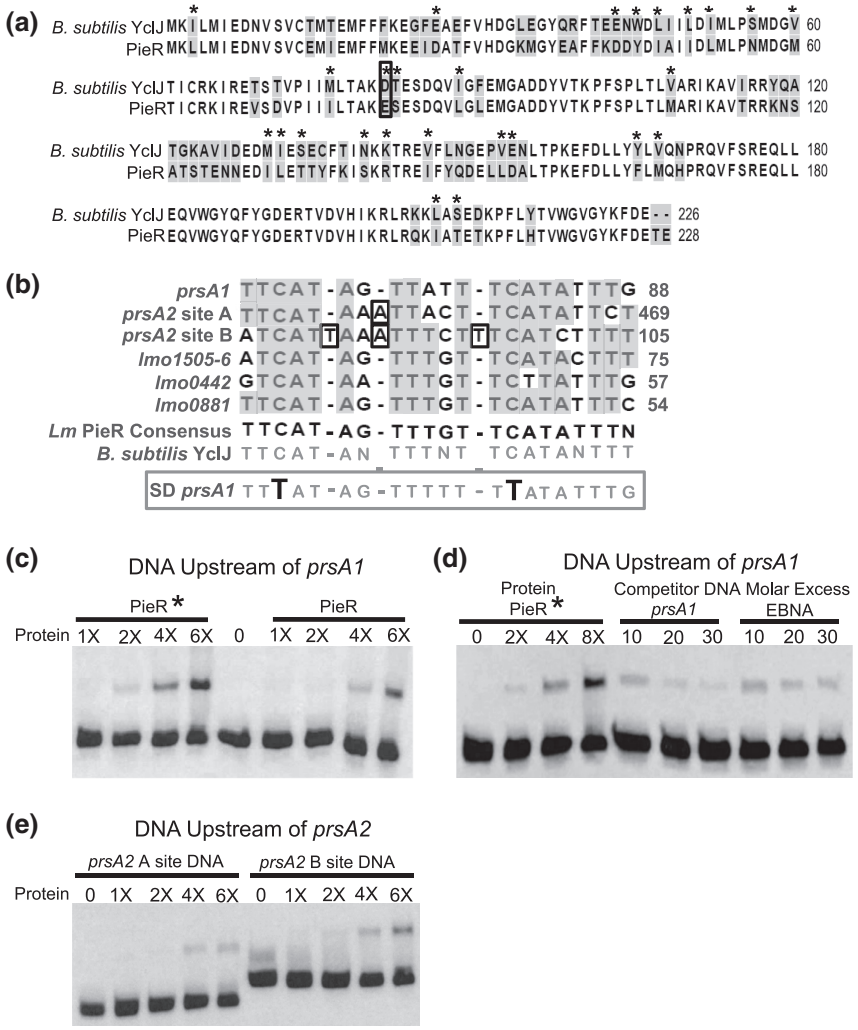

FIGURE 3 Sequence analysis and binding affinity of Lmo1507 (PieR). (a) PieR and *B. subtilis* orthologue YclJ. Alignment of *B. subtilis* YclJ and PieR indicates that the proteins are 71% identical and 82% similar. Amino acids that are not identical are shaded, while those that are similar are indicated by asterisks. The location of the E81V mutation is boxed. (b) a putative PieR binding consensus sequence. Each gene in the PieRS regulon contains one putative upstream PieR binding site where *prsA2* has two putative upstream binding sites. Base pair insertions are boxed in black. Numbers indicate location in base pairs upstream of the designated ATG start site of the gene or operon. The binding sequence for the PieR orthologue YclJ of *B. subtilis* is also shown and nucleotides that are identical to the YclJ binding sequence are shaded. A site directed *prsA1* PieR binding site mutant (SD*prsA1*) was constructed by mutating the two conserved cytosines to thymines (boxed in gray). (c) Electrophoretic mobility shift assay (EMSA) of PieR E81V (PieR*) and PieR binding to the DNA region upstream of *prsA1*. The relative binding affinity of increasing concentrations of PieR* and PieR where X is 15 pmol to 0.04 pmol of a labeled 109 base pair DNA region upstream of *prsA1* containing the putative PieR binding site. (d) EMSA shows that the interaction of PieR* with the DNA region upstream of *prsA1* is specific. The binding affinity of increasing concentrations of PieR* where X is 15 pmol to 0.04 pmol of labeled DNA upstream of *prsA1* is shown (as in C). The molar excess of unlabeled upstream *prsA1* competitor DNA and an irrelevant unlabeled competitor DNA, Epstein-Bar nuclear antigen (EBNA) is also shown. (e) EMSA of PieR* binding to DNA regions upstream of *prsA2*. The binding affinity of increasing concentrations of PieR* where X is 15 pmol to 0.04 pmol of a labeled 104 base pair region or 124 base pair region of DNA upstream of *prsA2* containing either the putative PieR binding site A or site B, respectively. Each EMSA shown is a representative of at least 3 independent experiments.

that increased levels of PrsA1 may have provided for the partial suppression of Δ*prsA2*-associated phenotypes. To determine the extent to which increased abundance of PrsA1 was compensating for the loss of PrsA2, a *prsA1* deletion was introduced into the Δ*prsA2 pieR** strain (Δ*prsA1* Δ*prsA2 pieR**). We further examined whether the PieR DNA binding site upstream of *prsA1* was required for the partial suppression of the Δ*prsA2* mutant phenotypes, and similarly investigated the phenotypes of strains completely lacking the *pieRS* encoded TCS (Δ*pieRS*).

The Δ*prsA2 pieR** strain recapitulated the partial suppression phenotypes observed for the original *prsA2* Targetron insertion mutant (*prsA2*::T) found to contain the *pieR** mutation (Figures 1 and 4). Increased expression of *prsA1* resulting from the *pieR** mutation restored secreted LLO and PC-PLC activity in Δ*prsA2* mutant backgrounds, and PrsA1-dependent restoration was eliminated by substitution of the two conserved cytosines with thymines within the PieR DNA binding site upstream of *prsA1* (SD

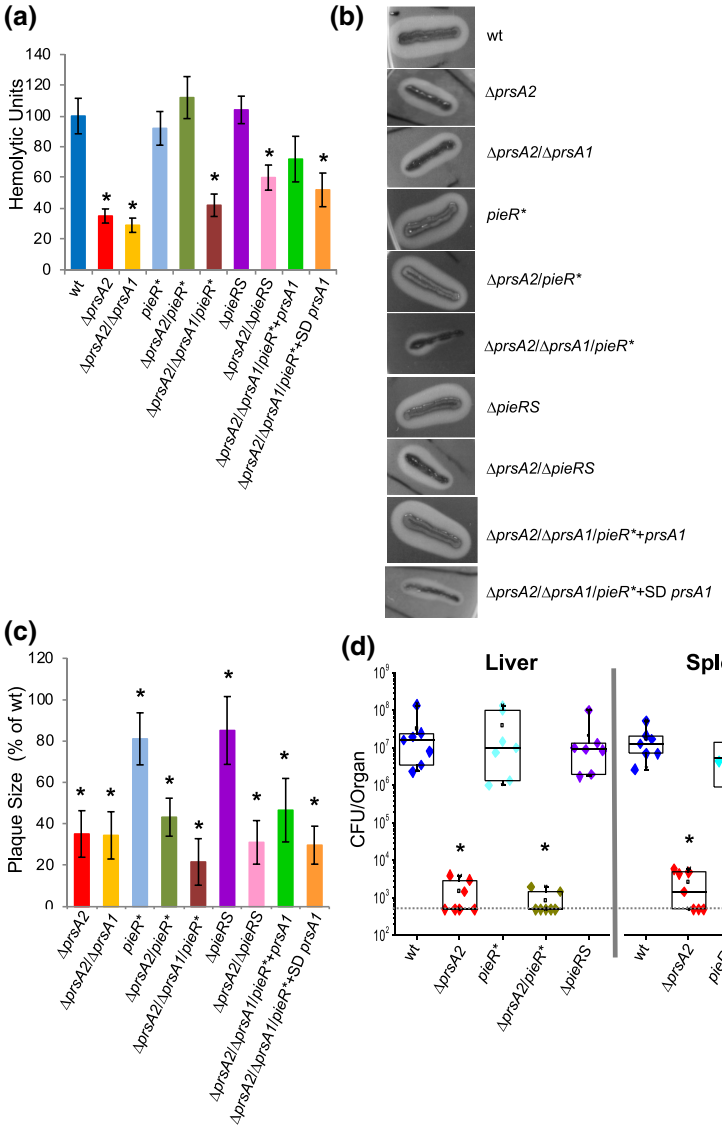

FIGURE 4 Analysis of bacterial virulence phenotypes. (a) Hemolytic activity. Dilutions of bacterial culture supernatants were assessed for their ability to lyse sheep RBCs. The reciprocal of the supernatant dilution that resulted in 50% RBC lysis (hemolytic units) was determined for 5 independent experiments. Error bars represent the standard error of the mean where $p \leq .05$ by two-tailed Student's T-test when compared to WT as indicated by an asterisks above bars. (b) Phospholipase activity. Strains were incubated on egg yolk agar plates, observation of a zone of opacity surrounding the bacterial streak is indicative of phospholipase activity, a representative is shown of four independent experiments. (c) Intracellular growth and cellular spread as measured by plaque assay. L2 fibroblast monolayers were infected with the indicated bacterial strain and plaque formation was determined in the presence of gentamicin 72 h post-infection. At least 20 plaques were measured in 3 independent experiments for all strains. Measurements represent plaque size with respect to WT (set at 100%). Error bars represent the standard error of the mean where $p \leq .05$ by two-tailed Student's T-test when compared to WT as indicated by an asterisks above bars. (d) Mouse bacterial burdens. Mice were infected with 2×10^4 colony forming units (CFUs) intravenously with the indicated strain. At 72 h post infection, bacterial burdens were determined in livers and spleens. Box plots are shown where each point represents one animal ($N = 7$) and a dotted line indicates the limit of detection. Asterisks above plots indicate statistical significance of $p \leq .05$ by two-tailed Wilcoxon rank-sum test when compared to WT.

prsA1, Figure 3b) (Figure 4a,b). The PieR* mutant and the Δ*pieRS* strain were similar to the wild-type strain in terms of secreted LLO and PC-PLC activity, suggesting that *pieRS* is not itself required for these activities and that the increased expression of *prsA1* resulting from PieR* was less functionally important in the presence of active PrsA2 (Figure 4a,b). All mutant strains lacking *prsA2* remained deficient for intracellular growth and cell-to-cell spread as measured by plaque formation in monolayers of L2 fibroblast cells (Figure 4c). The *pieR** mutant and the strain containing the full deletion of *pieRS* both exhibited slightly decreased plaque sizes suggesting that *pieRS* may have a minor role during the infection of cell monolayers (Figure 4c). However, there was no difference between wild type and the Δ*pieRS* mutant with respect to bacterial burdens in the livers and spleens of infected animals, a result that

indicates that *pieRS* is not required during intravenous infection of mice (Figure 4d).

To further delineate possible roles for the *pieRS* encoded TCS in *Lm* physiology, we examined bacterial growth under a number of conditions for which a requirement for PrsA2 activity has been previously demonstrated (Cahoon et al., 2016; Cahoon & Freitag, 2015). Growth of bacteria under acidic pH indicated that PrsA1 can compensate for the lack of PrsA2 in the presence of the *pieR** mutation (Figure 5a). Interestingly, the Δ*prsA2* Δ*prsA1 pieR** mutant exhibited less of a growth defect under low pH than the Δ*prsA2* Δ*prsA1* mutant suggesting that other genes within the PieRS regulon may be capable of compensating for the lack of PrsA2 (Figure 5a). *pieRS* is not itself required for bacterial survival under conditions of acidic pH (Figure 5a), suggesting that there may be redundant systems that contribute to resistance to acid stress. Under conditions of high osmolarity, the *pieR** mutation did not suppress the Δ*prsA2* sensitive phenotype nor was *pieRS* required for survival (Figure 5b). Bacterial motility was also not affected by the absence of *pieRS*, however PrsA1 was able to compensate for the lack of PrsA2 in the *pieR** background providing that the PieR DNA binding site upstream of *prsA1* was intact (Figure 5c).

Strains lacking PrsA2 exhibit increased sensitivity to antibiotics that target the bacterial cell wall (Alonzo et al., 2011; Cahoon & Freitag, 2015; Forster et al., 2011). We examined whether *pieRS* contributes to cell wall integrity by examining the minimum inhibitory concentrations of Δ*pieRS* mutants to penicillin and lysozyme. The Δ*pieRS* mutant exhibited similar patterns of growth to wild type strains in the presence of both penicillin and lysozyme (Figure 6a,b). PrsA1 contributes a minor role to penicillin resistance as the Δ*prsA2* Δ*prsA1* mutant was more sensitive to the drug than the Δ*prsA2* mutant (Figure 6a). However, increased expression of *prsA1* resulting from the presence of the *pieR** mutation did not compensate for the lack of PrsA2 in the presence of penicillin, although the suppressor mutation did enable PrsA1 to completely compensate for the lack of PrsA2 during growth in the presence of lysozyme (Figure 6a,b). We conclude that the *pieRS* encoded TCS is not required for bacterial survival in the presence of penicillin or lysozyme, however the *pieR** mutation provides sufficient PrsA1 to confer lysozyme resistance to Δ*prsA2* strains. The failure of increased PrsA1 expression to completely compensate for the lack of PrsA2 in the presence of penicillin suggests that PrsA2 may be uniquely required for the function of penicillin binding proteins.

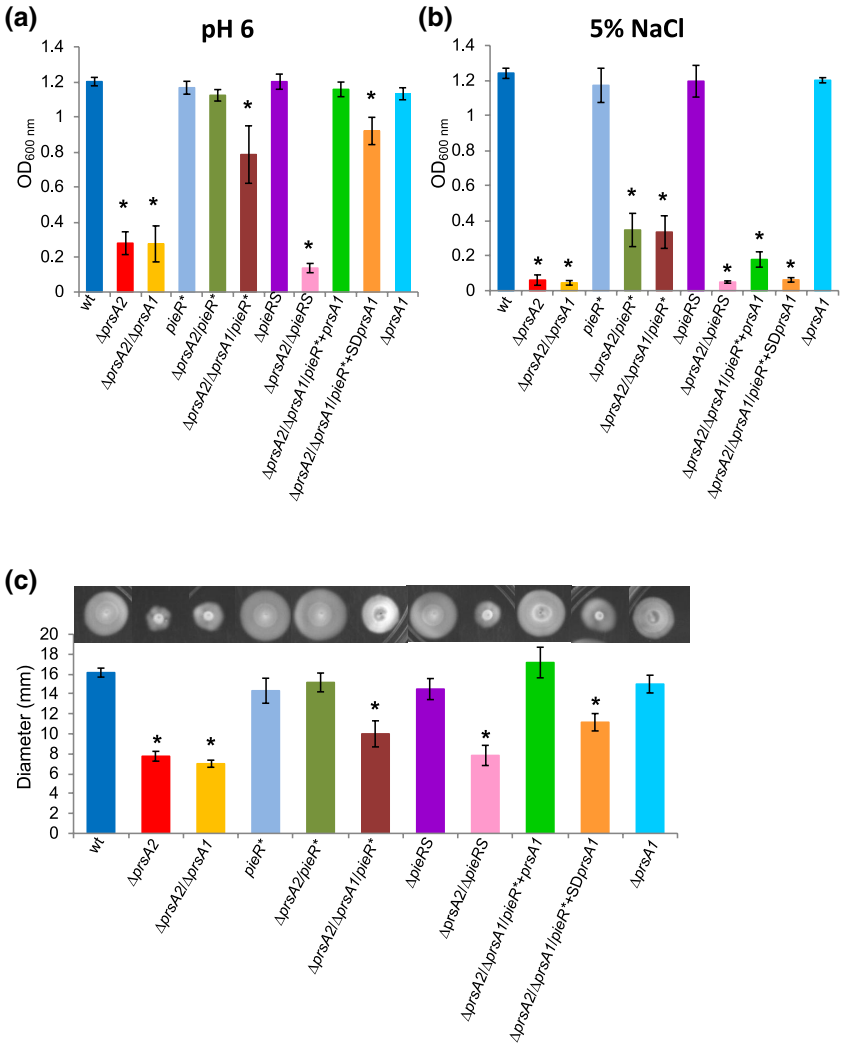

FIGURE 5 Analysis of cellular physiology phenotypes. (a) Growth at acidic pH. Growth is shown as optical density (OD_{600nm}) of strains inoculated from a saturated culture into liquid broth at pH 6 and grown overnight. Error bars represent the standard error of the mean for 3–6 experiments where $p \leq .05$ by two-tailed Student's T-test when compared to WT as indicated by an asterisks. (b) Growth at high osmolarity. Growth is shown as optical density (OD_{600nm}) of strains inoculated from a saturated culture into liquid broth containing 5% NaCl and grown overnight. Error bars represent the standard error of the mean for 6 experiments where $p \leq .05$ by two-tailed Student's T-test when compared to WT as indicated by an asterisks. (c) Swimming motility. The diameters of the swimming colonies are expressed as the average of 6–8 colonies from 3 independent experiments. Error bars represent the standard error of the mean where $p \leq .05$ by two-tailed Student's T-test when compared to WT as indicated by an asterisks.

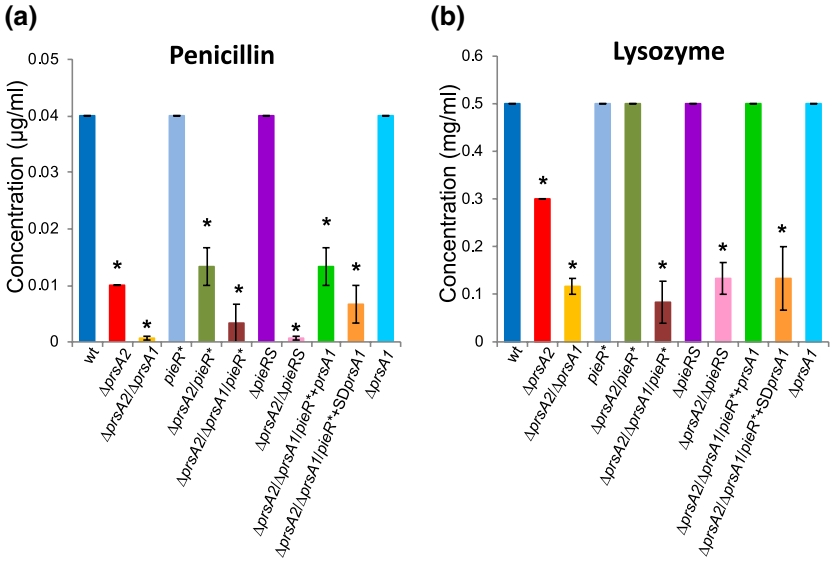

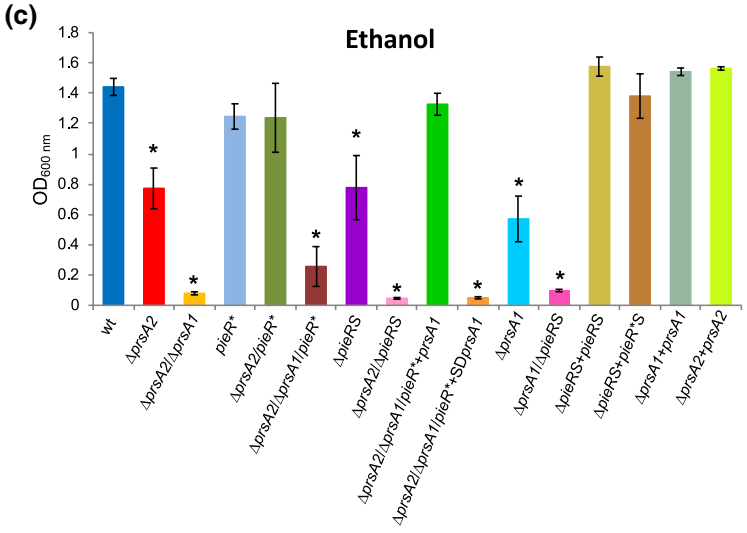

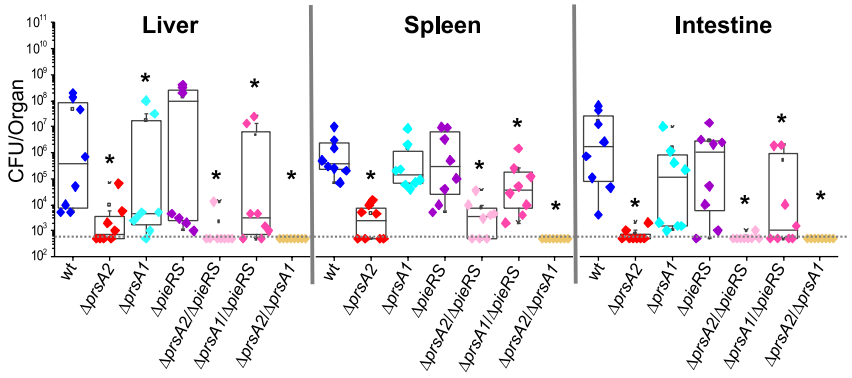

FIGURE 6 Contributions of the PrsA secretion chaperones and PieRS TCS to cell wall integrity and ethanol resistance. The minimum inhibitory concentration (MIC) to prevent growth was determined by bacterial inoculation into broth containing dilutions of the indicated cell wall active antibiotics. (a) the MIC of penicillin. (b) the MIC of lysozyme. Error bars represent the standard error of the mean of 4 cultures where $p \leq .05$ by two-tailed Student's T-test when compared to WT as indicated by an asterisks. (c) PieRS contributes to ethanol survival. Growth is shown as optical density (OD_{600nm}) of strains inoculated from a saturated culture into liquid broth containing 4% ethanol and grown overnight. Error bars represent the standard error of the mean of 4–8 independent cultures where $p \leq .05$ by two-tailed Student's T-test when compared to WT as indicated by an asterisks.

FIGURE 7 PieRS modulates *prsA1* and *prsA2* expression in the gut. Mice were infected orally by gastric gavage with 1×10^9 colony forming units (CFUs) with the indicated strains. At 72 h post-infection bacterial burdens were determined for livers, spleens, and intestines. Box plots are shown where each point represents one animal ($N = 8$). A dotted line indicates the limit of detection. Asterisks indicate statistical significance of $p \leq .05$, by two-tailed Wilcoxon rank-sum test when compared to WT.

2.5 | The PieRS TCS is required for ethanol resistance

An alternative form of cell stress can be manifested by exposure to ethanol which is known to modify lipid bilayers and cellular proteins (Konopasek et al., 2000; Silveira et al., 2004). Given that the secretion chaperones PrsA1 and PrsA2 reside at the membrane-cell wall interface and that the gene products are also part of the PieRS regulon, we assessed the effects of 4% ethanol exposure on strains lacking *pieRS*, *prsA1*, or *prsA2* (Figure 6c). Mutant strains lacking *pieRS*, *prsA1*,

or *prsA2* were all restricted for growth in the presence of ethanol, and each mutant could be successfully complemented by the introduction of the wild-type gene (Figure 6c). In addition, PrsA1 was able to fully compensate for the absence of PrsA2 in the presence of the *pieR** gain of function mutation and this suppression of the Δ*prsA2* defect required the presence of the PieR DNA binding site upstream of *prsA1* (Figure 6c). Analysis of the combined *pieR** Δ*prsA2* Δ*prsA1* mutant suggests that the other gene products encoded within the PieRS regulon at best have very minor roles during ethanol exposure when compared to PrsA1 and PrsA2 (Figure 7). In addition, the Δ*pieR* Δ*prsA2* and the Δ*pieRS* Δ*prsA1* mutants were found to be as sensitive to ethanol exposure as a Δ*prsA2* Δ*prsA1* double mutant indicating that activation of the *pieRS* TCS and the encoded chaperone activity are essential for bacterial survival following ethanol exposure (Figure 6c).

2.6 | The PieRS TCS is involved in *prsA1* and *prsA2* dependent survival in the gut

Ethanol exposure is a condition that interferes with protein folding and requires heightened chaperone activity at the membrane-cell wall interface; similar stresses on protein folding and cell membrane integrity are anticipated to be encountered by *Lm* during bacterial transit through the gastrointestinal tract. We therefore examined whether the *prsA1* and *prsA2* and possibly the *pieRS* gene products contribute to *Lm* survival following intragastric inoculation of mice, the natural route of *Lm* infection (Figure 7). Bacterial burdens in the intestine at 72 h post intragastric inoculation indicated that *prsA2* is essential for survival in the gut, whereas Δ*prsA1* and Δ*pieRS*-associated defects were only evident when combined (Δ*pieRS* Δ*prsA1*), indicating roles for PieRS, PrsA1 and PrsA2 during oral infection (Figure 7). In comparison to the Δ*pieRS* TCS mutant and the Δ*prsA1* single mutant, the bacterial burdens of Δ*pieRS* in combination with Δ*prsA1* were reduced during intragastric infection, indicating an additive effect. Following intestinal colonization, *Lm* translocates across the intestinal epithelium to distal organs such as the liver and spleen. As expected, bacterial burdens in the livers and spleens of infected animals were significantly reduced for Δ*prsA2* mutants as well as for Δ*prsA1* Δ*pieRS* mutants and Δ*prsA1* or Δ*pieRS* in combination with a *prsA2* deletion. Notably, Δ*prsA1* mutants were also significantly reduced in numbers in the liver but not within the intestine, suggesting that bacterial survival within the intestine was not significantly affected while bacterial translocation from the intestine to the liver was impaired (Figure 7). Taken together, these results suggest that *pieRS* TCS, *prsA1*, and *prsA2* contribute distinct and important roles during intragastric infection.

3 | DISCUSSION

The PrsA2 secretion chaperone has been shown to contribute to multiple aspects of *Lm* physiology and virulence, enabling *Lm* to survive under multiple stress conditions that likely interfere with protein folding at the membrane-cell wall interface. While PrsA2 activity is critical for *Lm* cell wall integrity, swimming motility, and the secretion of multiple virulence factors, the contributions of the related *Lm* secretion chaperone, PrsA1, have been less apparent. Here we show that PrsA2 and PrsA1 function together under the control of a two-component signal transduction system PieRS to enhance bacterial survival during intragastric infection and translocation across the intestinal epithelium to distal organs of mice. PrsA1 and PrsA2 occupy distinct roles during intragastric infection in that PrsA2 is necessary for intestinal colonization whereas PrsA1 is required for bacterial translocation across the intestine to reach the liver. The contributions of PieRS are somewhat more subtle, in that a mutant lacking the PieRS regulators is at best modestly compromised for bacterial virulence during intragastric infection. We interpret these findings to suggest that *prsA2* and *prsA1* are not exclusively regulated by PieRS during intragastric infection and that other regulatory mechanisms must exist for the induction of these critical chaperones in the GI tract.

The *pieR* E81V (*pieR**) mutation was fortuitously identified as gain of function mutation that led to the suppression of some but not all Δ*prsA2*-associated phenotypes. The presence of the *pieR** mutation resulted in the up-regulation of genes within the *pieRS* regulon including *prsA1* and *prsA2* (Figure 2b–D). We found that the suppression of many of the Δ*prsA2*-associated phenotypes was dependent on the presence of PrsA1 and required an intact PieR DNA binding site upstream of *prsA1*. With respect to PieRS regulon members outside of *prsA1* and *prsA2* and under the conditions tested thus far, only growth under acidic pH appeared to require the activity of other PieRS-regulated gene products in the absence of *prsA2* (Figure 5a). In addition, we identified one additional degenerate PieR binding site upstream of *htrA* which may account for the modest upregulation of *htrA*, ~1.44 Fold Log_2 and ~1.98 Fold Log_2 in the Δ*prsA2*/*pieR** and *pieR** strains, respectively. It is likely that the serine protease/chaperone HtrA may be induced and/or compensating for the loss of *prsA2* under acidic conditions as *htrA* has been previously shown to be required under conditions of acidic pH (Stack et al., 2005). It is also possible that other PieRS regulon members contribute to bacterial survival in the acidic gastric environment of the host following oral ingestion of *Lm*, however this remains to be determined. Based on the increased levels of gene expression of the PieRS regulon resulting from the PieR* mutation (Figure 2c,d) and the location and proximity of the PieR E81V mutation between the predicted phosphorylation site and residues important for phosphorylation mediated conformational changes (Figure S1b), we speculate that the PieR* mutation likely results in a conformational change that may mimic that which occurs following PieR phosphorylation, thereby increasing the affinity of PieR for its target DNA binding sites.

Given the importance of PrsA2 for multiple aspects of *Lm* physiology and virulence, it is perhaps not surprising that multiple regulators control *prsA2* expression. In addition to PieRS, *prsA2* expression is regulated by PrfA, the central regulator of *Lm* virulence gene

expression (Chatterjee et al., 2006; Port & Freitag, 2007) however binding of PrfA to the *prsA2* promoter does not appear to be required for virulence (Zemansky et al., 2009). The region upstream of *prsA1* does not have a recognizable PrfA binding site and loss of *prsA1* has no detectable effect on *Lm* bacterial virulence following intravenous infection of mice (Alonzo et al., 2009). Overall, our data indicate that PrsA2 acts as a multifaceted chaperone required for both intravenous and oral infections, whereas PrsA1 is required more selectively for bacterial transit from the intestine into distal organs such as the liver.

The regulation of *prsA1* and *prsA2* expression by PieRS represents the first genetic linkage identified between these two secretion chaperones. Based on in silico analysis and microarray data, the serine protease/chaperone encoded by *htrA* may also be modestly regulated by PieRS. Other Gram-positive *prsA* homologs have been shown to be activated by TCSs, such as *prsA* of *Streptococcus pneumoniae* (designated *ppmA*) which is activated by the TCS CiaRH that similarly activates the expression of *htrA* (Halfmann et al., 2007) and protects the cell from a variety of lysis-inducing conditions (Dagkessamanskaia et al., 2004; Mascher et al., 2006). The *prsA* of *Staphylococcus aureus* is regulated by the TCS VraRS and induced by cell wall stress (Jousselin et al., 2012). *S. pneumoniae* and *S. aureus* both have one *prsA* homolog whereas *Streptococcus pyogenes*, similar to *Lm*, has two *prsA* homologs; other Gram-positive bacteria have more (Cahoon & Freitag, 2014). Thus far the regulation of more than one *prsA* homolog by a single signaling system appears novel.

PieR appears to have a similar consensus DNA binding sequence to the *B. subtilis* orthologue YclJ (Ogura et al., 2010). *B. subtilis* TCS *yclJ-K* is induced under anaerobic conditions (Ye et al., 2000) whereas *pieRS* was not observed to be required under anaerobic conditions (data not shown). The response regulators, PieR and YclJ are more conserved than the sensor kinases, PieS and YclK, having 71% identity and 82% similarity versus 47% identity and 67% similarity, respectively. It seems likely that the amino acid differences in the sensor kinases may account for the difference in responses to external stimuli. The YclJ/YclK TCS is similar to the PieRS TCS in that both activate adjacent operons that have similar putative functions. YclJ/YclK activates *yclH/yclI* whereas PieRS activates *lmo1505-1506*, with each of these gene pairs encoding putative ABC-type transporter and permease proteins of an unknown substrate. Lmo1505 is 69% identical and 81% similar to YclH, whereas Lmo1506 is 58% identical and 72% similar to YclI. Whether these putative transporter proteins have similar functions and how function might contribute to stress resistance is unknown.

Previously, we observed that constitutive expression of *prsA1* in a Δ*prsA2* strain complemented many Δ*prsA2*-associated phenotypes (Cahoon & Freitag, 2015). Just as PrsA1 in the presence of the PieR* mutation suppressed the Δ*prsA2* associated swimming motility defect (Figure 5c), sensitivity to lysozyme (Figure 6b) and acidic pH (Figure 5a), so too could constitutive expression of PrsA1 complement these phenotypes in a Δ*prsA2* strain (Cahoon & Freitag, 2015). However constitutive expression of PrsA1 could also complement Δ*prsA2* sensitivity to penicillin and growth at high osmolarity (Cahoon & Freitag, 2015) whereas PrsA1 in the presence of the PieR* mutation did not (Figures 5b and 6a). There are many possible scenarios that may account for these differences: plasmid-associated constitutive expression of *prsA1* may be greater than the expression of *prsA1* in *pieR** background, penicillin and high osmolarity conditions may decrease the amount of PieR protein levels, other systems may regulate *prsA1* expression or PrsA1 protein translation under these conditions, or potentially the over-expression of the other gene products within the PieRS regulon in the absence of PrsA2 is somehow detrimental to the cell. Clarification awaits further experimentation.

Lm has 14 TCSs which are thought to respond to various stimuli to coordinate the expression of multiple genes (Glaser et al., 2001). There are likely redundancies among these systems that respond to specific signals or stresses. For example, similar to the TCS PieRS, the TCSs LisRK and CesRK and associated regulons are ethanol responsive (Nielsen et al., 2012). In contrast to PieRS, the absence of *lisRK* or *cesRK* resulted in enhanced growth of *Lm* in the presence of ethanol (Cotter et al., 1999; Kallipolitis et al., 2003; Kallipolitis & Ingmer, 2001; Williams et al., 2005). It is possible that other mechanisms compensate for the loss of either *lisRK* or *cesRK*, such as perhaps increased expression of the TCS PieRS regulon. There is only one gene product shared between the TCS PieRS and LisRK regulons, as both systems may regulate the expression of the serine protease/chaperone encoded by *htrA* (Nielsen et al., 2012; Stack et al., 2005). PieRS also regulates the expression of *lmo0442* encoding a fructose-specific PTS permease subunit IIA (Liu et al., 2017), whereas interestingly CesRK regulates the expression of the two genes surrounding *lmo0442* (Gottschalk et al., 2008; Kallipolitis et al., 2003). CesRK responsive elements have been identified upstream of *lmo0443* and *lmo0441* (Gottschalk et al., 2008) which encodes a fructose specific PTS permease subunit IIB (Liu et al., 2017) and a penicillin binding protein (Guinane et al., 2006), respectively. The *lmo0441* CesRK responsive element (Gottschalk et al., 2008) is within 37 base pairs of the PieR binding site upstream of *lmo442* (Figure 3b); whether the location of these sites relative to each other affects the expression of CesRK-regulated *lmo441* and PieRS-regulated *lmo442* is unknown.

We propose the following working model for the PieRS TCS (Figure 8). In the presence of ethanol or under forms of gastric stress, the sensor kinase PieS activates the response regulator PieR which in turn leads to the activation of *prsA1*, *prsA2*, and potentially the other genes of the *pieRS* regulon. Ethanol attacks lipid bilayers and causes the unfolding of proteins (Konopasek et al., 2000; Silveira et al., 2004); the up-regulation of the molecular chaperones PrsA1 and PrsA2 is a likely stress response necessary to maintain proper protein folding at the cell membrane-cell wall interface as well as normal protein secretion (Figure 8). Since ethanol elicits protein unfolding, we hypothesize that similar stress conditions very likely exist in the host gastrointestinal tract that result in protein unfolding

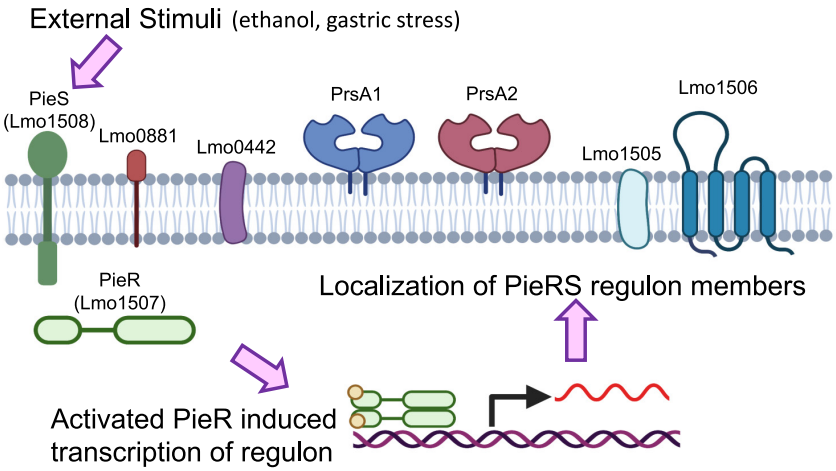

FIGURE 8 Model of PieRS regulation. An external stimulus activates the sensor kinase PieS that activates the cognate response regulator PieR which induces expression of the PieRS regulon. Genes associated with the PieRS regulon include *prsA1*, *prsA2*, *lmo1505-lmo1506*, *lmo0442*, and *lmo0881*. PrsA1 and PrsA2 are PPIase secretion chaperones. Lmo1507 and Lmo1506 are a putative ABC transporter ATP-binding protein and a putative macrolide ABC transporter permease, respectively. Lmo0442 is a putative fructose specific phosphotransferase transport system (PTS) component permease whereas the function of Lmo0881 is unknown. The localization of the PieRS regulon members is indicated.

and require the apparently distinct activities of both PrsA secretion chaperones, thus enhancing bacterial survival and the ability to translocate across the intestinal epithelium to deeper tissues and distal organs.

4 | MATERIALS AND METHODS

4.1 | Bacterial strains, plasmids, and media

Bacterial strains used in this study are listed in Supplemental Table S1. *Lm* 10403S is the wild-type (WT) strain and Δ*prsA2* is *Lm* 10403S containing an erythromycin resistance gene (*erm*) in place of the *prsA2* coding sequence (Alonzo et al., 2009), while Δ*prsA1* transduced with Δ*prsA2*::*erm* is Δ*prsA2* Δ*prsA1* (Alonzo & Freitag, 2010). The original *prsA2* suppressor mutant (*prsA2*::T) contains a targeted insertional disruption of *prsA2* that was generated by using the Targetron gene knockout system (Sigma) (Alonzo et al., 2009). *Escherichia coli* One Shot TOP10 (Invitrogen), SM10, and S17 (a kind gift from N. Cianciotto, Northwestern University) were used as host strains for recombinant plasmids, whereas *E. coli* BL21-CodonPlus (DE3)-RIL cells was used for protein expression. *E. coli* and *Lm* were grown in Luria broth (LB) or terrific broth (TB) and brain heart infusion (BHI) medium, respectively. The integration plasmid pPL2 (Lauer et al., 2002) was used for genetic complementation of *lmo1507* E81V Δ*prsA2* Δ*prsA1* with *prsA1* or SD*prsA1* (Figure 3c) while the integration plasmid pIMK2 (Monk et al., 2008) (a kind gift from C. Hill, Cork College) was used for complementation of Δ*lmo1507/1508* with *lmo1507/1508*, Δ*lmo1507/1508* with *lmo1507* E81V-*1508*, Δ*prsA1* with *prsA1*, and Δ*prsA2* with *prsA2* (Cahoon & Freitag, 2015). The N-terminal His-tagged plasmid pQE30 (Qiagen) was used for protein expression of Lmo1507 and Lmo1507 E81V in *E. coli*.

4.2 | Whole genome sequencing of the *prsA2*::T strain

Genomic DNA from the prsA2::T strain was isolated (Qiagen) and sequenced using the SOLiD DNA sequencing system at the University of Oklahoma Health Sciences Center. Reads were aligned to the genome of *Listeria monocytogenes* 10,403s using CLC Genomics Workbench to determine nucleotide differences.

4.3 | Construction of the *lmo1507/1508* mutant strains

To generate *lmo1507* E81V, a fragment containing the encoded E81V mutation was PCR amplified from *prsA2*::T genomic DNA using primers designed with a BamHI and SacI restriction site, lmo1507F2-BamHI and lmo1507R2-SacI, respectively (Supplemental Table S2). The fragment was cloned into the shuttle vector pKSV7 and used for allelic exchange in strains WT, Δ*prsA2*, and Δ*prsA2* Δ*prsA1* as previously described (Camilli et al., 1993). The Δ*lmo1507/1508* in frame deletion was constructed by splicing by overlap extension (SOE) PCR (Horton, 1993). Two DNA fragments were generated by PCR using primers 1507F1BamHIpA/ 1507KpnI1508pB and 1508R1SacIpD/1507KpnI1508pC (Supplemental Table S2) with genomic DNA from *Lm* 10403S. The two fragments were gel purified (Qiagen) and PCR amplified using primer pair 1507F1BamHIpA/1508R1SacIpD to generate a ~ 1520 bp product encompassing the upstream and downstream region of *lmo1507/1508*. This fragment was cloned into the shuttle vector pKSV7 and introduced for allelic exchange into WT, Δ*prsA2*, Δ*prsA1* and Δ*prsA2* Δ*prsA1* as previously described (Camilli et al., 1993). To generate *prsA1* complemented strains, the region encompassing 195 bp upstream and 66 bp

downstream of *prsA1* was amplified with primers PrsA1UPSacF1/PrsA1XmaR2 (Supplemental Table S2) from *Lm* 10,403s genomic DNA and cloned into the integration plasmid pPL2 (Lauer et al., 2002); to generate the SD*prsA1* strain, this construct was mutated with a site directed mutagenesis kit (Agilent Technologies) and primers listed in Supplemental Table S2. Each plasmid was transformed into SM10 cells and allowed to integrate into *Lm* 1507 E81V Δ*prsA2* Δ*prsA1* by conjugation. The *lmo1507/1508* and *lmo1507* E81V-1508 complementation strains were generated by amplification of a region 257 bp upstream of *lmo1507* and 180 bp downstream of *lmo1508* from *Lm* 10,403s or *Lm1507* E81V genomic DNA, respectively, and cloned into the integration plasmid pIMK2 (Monk et al., 2008). These constructs were transformed into S17 cells and delivered to integrate into Δ*lmo1507/1508* by conjugation.

4.4 | Construction and purification of recombinant Lmo1507 and Lmo1507 E81V

The DNA sequence corresponding to Lmo1507 and Lmo1507 E81V was amplified from *Lm* 10,403s or *prsA2*::T genomic DNA with primers designed with a SacI and XmaI restriction site, lm1507F-1SacEx and lm1507R1XmaEx, respectively. The fragment was cloned into the N-terminal His-tagged pQE30 expression system (Qiagen). *E. coli* BL21-CodonPlus (DE3)-RIL cells (Stratagene) were used for recombinant Lmo1507 and Lmo1507 E81V expression. Two liters of TB medium was inoculated with a 1:100 dilution of the appropriate overnight culture. Cells were grown at 37 °C until reaching an OD600 of 0.9. The temperature was then lowered to 25 °C and Lmo1507 expression was induced by the addition of isopropyl-1-thio-D-galactopyranoside to a final concentration of 0.5 mM. The next morning, cells were collected by centrifugation and resuspended in sample buffer [10 mM Tris–HCl pH 8.3, 500 mM NaCl and 1 mM tris(2-carboxyethyl)phosphine] supplemented with 10% glycerol. Cells were lysed by sonication and the cellular lysate was cleared by centrifugation. The soluble fraction of the lysate was loaded onto a 5 ml HisTrap FF nickel column (GE Healthcare Life Sciences) and washed with wash buffer (sample buffer supplemented with 25 mM imidazole). His-tagged Lmo1507 or Lmo1507 E81V was eluted with elution buffer (sample buffer supplemented with 500 mM imidazole). The eluant was immediately injected onto a HiPrep 26/60 Superdex size-exclusion column (GE Healthcare Life Sciences) that had been pre-equilibrated with sample buffer. A single peak eluted from the size-exclusion column and was confirmed to contain homogenous Lmo1507 or Lmo1507 E81V by SDS-PAGE.

4.5 | Electrophoretic mobility shift assay (EMSA)

Putative binding sites from *prsA1* and *prsA2* were PCR amplified from the *Lm* genomic DNA with primers containing a biotin tag at the 3′ end using Phusion HF DNA polymerase (Biolabs). The resulting PCR product was run on a 0.8% agarose gel and purified using Qiaquick gel extraction kit (Qiagen). The gel shift assay was performed according to the instructions in the LightShift EMSA Optimization and Control Kit (Thermo Scientific) with the contents added in the following order to a final reaction volume of 10 µl: ultrapure water (variable), 10X binding buffer (1X), 50% glycerol (2.5%), 100 mM $MgCl_2$ (5 mM), 1 µg/µl Poly (dI.dC) (50 ng/µl), 1% NP-40 (0.05%), unlabeled DNA, respective protein and labeled DNA (40 fmol). The reactions were then incubated for 20 min at room temperature (RT) before loading the entire volume onto a pre-run (30 min in chilled 0.5X TBE, 100 V) 5% PAGE gel and ran in chilled 0.5X TBE at 100 V. The binding reactions were then transferred onto a nylon membrane (Millipore) at 280–300 mA for 60 min. The transferred DNA was then crosslinked to the membrane using UV-light (120 mJ/cm^2) for 45–50 s followed by detection of the biotin labeled DNA by using the Chemiluminescent Nucleic Acid detection module (Thermo Scientific). In experiments where unlabeled DNA was used, the reaction was first incubated with protein and unlabeled DNA for 20 min at RT, followed by incubation with labeled DNA for 20 min at RT.

4.6 | Swimming motility assay

To assess swimming motility, mid-log phase (OD_{600nm} ~0.8) cultures (2 µl) were inoculated into soft BHI agar (0.3%) plates and grown at 37°C for 24 h and subsequently at 25°C for 24 h. Motility was measured as the diameter of the spreading colony in at least 5 independent experiments.

4.7 | Hemolysin assays

Hemolytic activity was measured as previously described (Cahoon & Freitag, 2015). Briefly, bacterial cultures were grown overnight in LB, diluted 1:10 in fresh media and grown for 5 h. Culture supernatants were normalized to equivalent OD_{600} values and serially diluted into PBS pH 5 containing 1 mM DTT (PBS-DTT) and incubated at 37°C for 30 min. Subsequently, 100 µl of a 1:5 dilution of PBS-DTT washed sheep red blood cells (RBCs) was added and incubated for 30 min at 37°C. Bacterial supernatant/RBCs mixtures were pelleted and the supernatant dilution resulting in 50% RBC lysis was determined by visual inspection of the pellet.

4.8 | Detection of phospholipase activity

Phospholipase activity was detected using Brilliance *Listeria* Agar with differential supplement containing lecithin (Oxoid). An opaque halo around the bacterial streak is produced upon *Lm* phospholipase hydrolysis of lecithin in the medium. Single colonies were struck onto the medium and incubated for 24 h at 37°C followed by visual inspection of the zone of opacity surrounding the bacterial streaks.

4.9 | Intravenous and oral mouse infections

Animal procedures were approved by the UIC Animal Care Committee and were conducted in the Biological Resources Laboratory following AAALAC approved procedures and guidelines. Overnight cultures were diluted 1:20 in BHI broth and grown to mid-log phase and normalized based on OD_{600} values, washed twice with PBS pH 7, diluted, and re-suspended in PBS pH 7. For intravenous infections, female 7–9 week old Swiss Webster mice (Charles River Laboratories) were injected with 200 µl containing $2x10^4$ CFU of bacteria by tail vein injection, whereas for oral infections, mice were infected with 200 µl containing $1x10^9$ CFU of bacteria by gastric gavage. For competitive intravenous and oral infections, a 1:1 mixture or reference strain DP-3903 (Auerbuch et al., 2001) to test strain was used totaling $2x10^4$ CFU and $1x10^9$ CFU, respectively. At 72 h post infection, organs of infected animals were collected, homogenized, and 10-fold serial dilutions were plated for total CFUs.

4.10 | L2 plaque assays

Plaque assays were conducted as previously described (Sun et al., 1990). Briefly, in 6-well culture dishes monolayers of L2 mouse fibroblasts were infected at an MOI of 30:1 for 1 h. Subsequently, infected monolayers were washed three times with PBS pH 7 and overlaid with DMEM/agarose containing 10 µg/ml gentamicin to kill extracellular bacteria. At 72 h, plaques were measured with a micrometer.

4.11 | Growth assays under conditions of acidic pH, high osmolarity, and in ethanol

For growth assays, 2 µl of a saturated overnight culture was inoculated into 2 ml BHI liquid broth at pH 6 (acidic pH), containing 5% NaCl w/v (high osmolarity), or 4% ethanol. Cultures were grown overnight at 37°C with agitation and growth was measured as a function of optical density (OD_{660nm}).

4.12 | Determination of antibiotic minimum inhibitory concentration

To determine the MIC, 2 µl of a mid-log phase (OD600nm ~0.8) culture was inoculated into 2 ml BHI broth in 4 ml polypropylene tubes containing dilutions of penicillin G or lysozyme. Cultures were grown with agitation at 37°C for 16 h followed by visual inspection where the MIC was noted as the complete inhibition of bacterial growth.

4.13 | RNA extraction, microarray and qRT-PCR analysis

Lm overnight cultures were diluted 1:20 in BHI broth and grown to an OD_{600nm} ~0.6. Bacteria were normalized based on OD_{600} values and ~7 ml was collected for each strain then 1 volume of RNAprotect Bacteria Reagent (Qiagen) was added. Bacteria were recovered by centrifugation and treated with 20 mg/ml lysozyme and 50 mg/ml *Lm* endolysin in TE pH 8 in a total volume of 1 ml for 15 min at 37°C, vortexing every 5 min. Then pellets were sonicated on ice for 30 s followed by incubation on ice for 30 s; this was repeated an additional 4 times. RNA extraction was performed using the RNeasy Mini Kit (Qiagen) with on-column DNAse digestion. DNA microarrays were performed using extracted RNA by Microarrays Inc. Three independent microarrays were performed for each strain where each microarray contained 3 spots per gene; microarray values were averaged and normalized with RpoB. For qRT-PCR, both cDNA synthesis and qPCR was performed by the UIC Research Resources Center DNA Services Facility. Three independent RNA replicates were quantified 3 times each and normalized to RpoB. A no template control was included for each primer/probe set and no-reverse transcriptase control was include for each RNA sample and primer/probe set. Gene specific primer pairs and probes were generated using the IDT Prime Time Custom qPCR Probes application and purchased from the manufacture premixed in a 20 µl volume at a ratio of 1:1:0.5 nanomoles of forward primer to reverse primer to probe, respectively (Integrated DNA Technologies). For qPCR reactions, TaqMan gene expression master mix (Applied Biosystems) was used as specified by the manufacture with 2 µl of a 1:10 dilution of the premixed primer/probe in a final reaction volume of 20 µl. Fold changes were determined using the comparative $2^{\Delta\Delta CT}$ method (Schmittgen & Livak, 2008).

4.14 | Statistical analyses

A two-tailed Student's T-test was used for statistical analysis where $p \leq .05$ and error bars represent the standard error of the mean for data represented as a bar graph. A two-tailed Wilcoxon Rank-Sum Test was used where $p \leq .05$ for data represented as box plots.

ACKNOWLEDGEMENT

We thank members of the Freitag laboratory and the UIC Positive Thinking group for helpful discussions. This work was supported by NIH grants R01 AI083241 and AI083241-03S1 to NEF and NRSA F32 AI115954-01 to LAC. Its contents are solely the responsibility of the authors and do not necessarily represent the official views of the funding source.

DATA AVAILABILITY STATEMENT

The data that support the findings of this study are openly available in https://doi.org/10.6084/m9.figshare.19723630.v1.

ORCID

Avinash N. Gururaja https://orcid.org/0000-0002-7500-9670
Nancy E. Freitag https://orcid.org/0000-0003-1322-3978

REFERENCES

Ahmed, J.K. & Freitag, N.E. (2016) Secretion chaperones PrsA2 and HtrA are required for listeria monocytogenes replication following

intracellular induction of virulence factor secretion. *Infection and Immunity*, *84*, 3034–3046.

Alonzo, F., 3rd & Freitag, N.E. (2010) Listeria monocytogenes PrsA2 is required for virulence factor secretion and bacterial viability within the host cell cytosol. *Infection and Immunity*, *78*, 4944–4957.

Alonzo, F., 3rd, Port, G.C., Cao, M. & Freitag, N.E. (2009) The post-translocation chaperone PrsA2 contributes to multiple facets of listeria monocytogenes pathogenesis. *Infection and Immunity*, *77*, 2612–2623.

Alonzo, F., 3rd, Xayarath, B., Whisstock, J.C. & Freitag, N.E. (2011) Functional analysis of the listeria monocytogenes secretion chaperone PrsA2 and its multiple contributions to bacterial virulence. *Molecular Microbiology*, *80*, 1530–1548.

Altschul, S.F., Gish, W., Miller, W., Myers, E.W. & Lipman, D.J. (1990) Basic local alignment search tool. *Journal of Molecular Biology*, *215*, 403–410.

Auerbuch, V., Lenz, L.L. & Portnoy, D.A. (2001) Development of a competitive index assay to evaluate the virulence of listeria monocytogenes actA mutants during primary and secondary infection of mice. *Infection and Immunity*, *69*, 5953–5957.

Cahoon, L.A. & Freitag, N.E. (2014) Listeria monocytogenes virulence factor secretion: don't leave the cell without a chaperone. *Frontiers in Cellular and Infection Microbiology*, *4*, 13.

Cahoon, L.A. & Freitag, N.E. (2015) Identification of conserved and species-specific functions of the listeria monocytogenes PrsA2 secretion chaperone. *Infection and Immunity*, *83*, 4028–4041.

Cahoon, L.A., Freitag, N.E. & Prehna, G. (2016) A structural comparison of listeria monocytogenes protein chaperones PrsA1 and PrsA2 reveals molecular features required for virulence. *Molecular Microbiology*, *101*, 42–61.

Camilli, A., Tilney, L.G. & Portnoy, D.A. (1993) Dual roles of plcA in listeria monocytogenes pathogenesis. *Molecular Microbiology*, *8*, 143–157.

Chatterjee, S.S., Hossain, H., Otten, S., Kuenne, C., Kuchmina, K., Machata, S. et al. (2006) Intracellular gene expression profile of listeria monocytogenes. *Infection and Immunity*, *74*, 1323–1338.

Cotter, P.D., Emerson, N., Gahan, C.G. & Hill, C. (1999) Identification and disruption of lisRK, a genetic locus encoding a two-component signal transduction system involved in stress tolerance and virulence in listeria monocytogenes. *Journal of Bacteriology*, *181*, 6840–6843.

Dagkessamanskaia, A., Moscoso, M., Henard, V., Guiral, S., Overweg, K., Reuter, M. et al. (2004) Interconnection of competence, stress and CiaR regulons in Streptococcus pneumoniae: competence triggers stationary phase autolysis of ciaR mutant cells. *Molecular Microbiology*, *51*, 1071–1086.

de las Heras, A., Cain, R.J., Bielecka, M.K. & Vazquez-Boland, J.A. (2011) Regulation of listeria virulence: PrfA master and commander. *Current Opinion in Microbiology*, *14*, 118–127.

Forster, B.M., Zemansky, J., Portnoy, D.A. & Marquis, H. (2011) Posttranslocation chaperone PrsA2 regulates the maturation and secretion of listeria monocytogenes proprotein virulence factors. *Journal of Bacteriology*, *193*, 5961–5970.

Freitag, N.E., Youngman, P. & Portnoy, D.A. (1992) Transcriptional activation of the listeria monocytogenes hemolysin gene in *Bacillus subtilis*. *Journal of Bacteriology*, *174*, 1293–1298.

Freitag, N.E., Port, G.C. & Miner, M.D. (2009) Listeria monocytogenes - from saprophyte to intracellular pathogen. *Nature Reviews. Microbiology*, *7*, 623–628.

Glaser, P., Frangeul, L., Buchrieser, C., Rusniok, C., Amend, A., Baquero, F. et al. (2001) Comparative genomics of listeria species. *Science*, *294*, 849–852.

Gottschalk, S., Bygebjerg-Hove, I., Bonde, M., Nielsen, P.K., Nguyen, T.H., Gravesen, A. et al. (2008) The two-component system CesRK controls the transcriptional induction of cell envelope-related genes in listeria monocytogenes in response to cell wall-acting antibiotics. *Journal of Bacteriology*, *190*, 4772–4776.

Guinane, C.M., Cotter, P.D., Ross, R.P. & Hill, C. (2006) Contribution of penicillin-binding protein homologs to antibiotic resistance, cell morphology, and virulence of listeria monocytogenes EGDe. *Antimicrobial Agents and Chemotherapy*, *50*, 2824–2828.

Halfmann, A., Kovacs, M., Hakenbeck, R. & Bruckner, R. (2007) Identification of the genes directly controlled by the response regulator CiaR in Streptococcus pneumoniae: five out of 15 promoters drive expression of small non-coding RNAs. *Molecular Microbiology*, *66*, 110–126.

Hernandez-Milian, A. & Payeras-Cifre, A. (2014) What is new in listeriosis? *BioMed Research International*, *2014*, 358051.

Horton, R.M. (1993) In vitro recombination and mutagenesis of DNA: SOEing together tailor-made genes. *Methods in Molecular Biology*, *15*, 251–261.

Jousselin, A., Renzoni, A., Andrey, D.O., Monod, A., Lew, D.P. & Kelley, W.L. (2012) The posttranslocational chaperone lipoprotein PrsA is involved in both glycopeptide and oxacillin resistance in *Staphylococcus aureus*. *Antimicrobial Agents and Chemotherapy*, *56*, 3629–3640.

Kallipolitis, B.H. & Ingmer, H. (2001) Listeria monocytogenes response regulators important for stress tolerance and pathogenesis. *FEMS Microbiology Letters*, *204*, 111–115.

Kallipolitis, B.H., Ingmer, H., Gahan, C.G., Hill, C. & Sogaard-Andersen, L. (2003) CesRK, a two-component signal transduction system in listeria monocytogenes, responds to the presence of cell wall-acting antibiotics and affects beta-lactam resistance. *Antimicrobial Agents and Chemotherapy*, *47*, 3421–3429.

Kelley, L.A., Mezulis, S., Yates, C.M., Wass, M.N. & Sternberg, M.J. (2015) The Phyre2 web portal for protein modeling, prediction and analysis. *Nature Protocols*, *10*, 845–858.

Kobayashi, K., Ogura, M., Yamaguchi, H., Yoshida, K., Ogasawara, N., Tanaka, T. et al. (2001) Comprehensive DNA microarray analysis of *Bacillus subtilis* two-component regulatory systems. *Journal of Bacteriology*, *183*, 7365–7370.

Konopasek, I., Strzalka, K. & Svobodova, J. (2000) Cold shock in *Bacillus subtilis*: different effects of benzyl alcohol and ethanol on the membrane organisation and cell adaptation. *Biochimica et Biophysica Acta*, *1464*, 18–26.

Lauer, P., Chow, M.Y., Loessner, M.J., Portnoy, D.A. & Calendar, R. (2002) Construction, characterization, and use of two listeria monocytogenes site-specific phage integration vectors. *Journal of Bacteriology*, *184*, 4177–4186.

Leimeister-Wachter, M., Haffner, C., Domann, E., Goebel, W. & Chakraborty, T. (1990) Identification of a gene that positively regulates expression of listeriolysin, the major virulence factor of listeria monocytogenes. *Proceedings of the National Academy of Sciences of the United States of America*, *87*, 8336–8340.

Liu, Y., Yoo, B.B., Hwang, C.A., Suo, Y., Sheen, S., Khosravi, P. et al. (2017) LMOf2365_0442 encoding for a fructose specific PTS Permease IIA may be required for virulence in L. monocytogenes strain F2365. *Frontiers in Microbiology*, *8*, 1611.

Lomonaco, S., Nucera, D. & Filipello, V. (2015) The evolution and epidemiology of listeria monocytogenes in Europe and the United States. *Infection, Genetics and Evolution*, *35*, 172–183.

Lu, S., Wang, J., Chitsaz, F., Derbyshire, M.K., Geer, R.C., Gonzales, N.R. et al. (2020) CDD/SPARCLE: the conserved domain database in 2020. *Nucleic Acids Research*, *48*, D265–D268.

Lund, B.M. (2015) Microbiological food safety for vulnerable people. *International Journal of Environmental Research and Public Health*, *12*, 10117–10132.

Mascher, T., Heintz, M., Zahner, D., Merai, M. & Hakenbeck, R. (2006) The CiaRH system of *Streptococcus pneumoniae* prevents lysis during stress induced by treatment with cell wall inhibitors and by

mutations in pbp2x involved in beta-lactam resistance. *Journal of Bacteriology*, *188*, 1959–1968.
Mengaud, J., Dramsi, S., Gouin, E., Vazquez-Boland, J.A., Milon, G. & Cossart, P. (1991) Pleiotropic control of listeria monocytogenes virulence factors by a gene that is autoregulated. *Molecular Microbiology*, *5*, 2273–2283.
Mistry, J., Chuguransky, S., Williams, L., Qureshi, M., Salazar, G.A., Sonnhammer, E.L.L. et al. (2021) Pfam: the protein families database in 2021. *Nucleic Acids Research*, *49*, D412–D419.
Monk, I.R., Gahan, C.G. & Hill, C. (2008) Tools for functional postgenomic analysis of listeria monocytogenes. *Applied and Environmental Microbiology*, *74*, 3921–3934.
Mostowy, S. & Cossart, P. (2012) Virulence factors that modulate the cell biology of listeria infection and the host response. *Advances in Immunology*, *113*, 19–32.
Mueller, K.J. & Freitag, N.E. (2005) Pleiotropic enhancement of bacterial pathogenesis resulting from the constitutive activation of the listeria monocytogenes regulatory factor PrfA. *Infection and Immunity*, *73*, 1917–1926.
Nielsen, P.K., Andersen, A.Z., Mols, M., van der Veen, S., Abee, T. & Kallipolitis, B.H. (2012) Genome-wide transcriptional profiling of the cell envelope stress response and the role of LisRK and CesRK in listeria monocytogenes. *Microbiology*, *158*, 963–974.
Ogura, M., Tsukahara, K. & Tanaka, T. (2010) Identification of the sequences recognized by the Bacillus subtilis response regulator YclJ. *Archives of Microbiology*, *192*, 569–580.
Port, G.C. & Freitag, N.E. (2007) Identification of novel listeria monocytogenes secreted virulence factors following mutational activation of the central virulence regulator, PrfA. *Infection and Immunity*, *75*, 5886–5897.
Sarvas, M., Harwood, C.R., Bron, S. & van Dijl, J.M. (2004) Post-translocational folding of secretory proteins in gram-positive bacteria. *Biochimica et Biophysica Acta*, *1694*, 311–327.
Schmittgen, T.D. & Livak, K.J. (2008) Analyzing real-time PCR data by the comparative C(T) method. *Nature Protocols*, *3*, 1101–1108.
Shetron-Rama, L.M., Mueller, K., Bravo, J.M., Bouwer, H.G., Way, S.S. & Freitag, N.E. (2003) Isolation of listeria monocytogenes mutants with high-level in vitro expression of host cytosol-induced gene products. *Molecular Microbiology*, *48*, 1537–1551.
Silveira, M.G., Baumgartner, M., Rombouts, F.M. & Abee, T. (2004) Effect of adaptation to ethanol on cytoplasmic and membrane protein profiles of Oenococcus oeni. *Applied and Environmental Microbiology*, *70*, 2748–2755.
Stack, H.M., Sleator, R.D., Bowers, M., Hill, C. & Gahan, C.G. (2005) Role for HtrA in stress induction and virulence potential in listeria monocytogenes. *Applied and Environmental Microbiology*, *71*, 4241–4247.
Sun, A.N., Camilli, A. & Portnoy, D.A. (1990) Isolation of Listeria monocytogenes small plaque mutants defective for intracellular growth and cell-to-cell spread. *Infection and Immunity*, *58*, 3770–3778.
van Wely, K.H., Swaving, J., Freudl, R. & Driessen, A.J. (2001) Translocation of proteins across the cell envelope of gram-positive bacteria. *FEMS Microbiology Reviews*, *25*, 437–454.
Williams, T., Bauer, S., Beier, D. & Kuhn, M. (2005) Construction and characterization of listeria monocytogenes mutants with in-frame deletions in the response regulator genes identified in the genome sequence. *Infection and Immunity*, *73*, 3152–3159.
Ye, R.W., Tao, W., Bedzyk, L., Young, T., Chen, M. & Li, L. (2000) Global gene expression profiles of *Bacillus subtilis* grown under anaerobic conditions. *Journal of Bacteriology*, *182*, 4458–4465.
Zemansky, J., Kline, B.C., Woodward, J.J., Leber, J.H., Marquis, H. & Portnoy, D.A. (2009) Development of a mariner-based transposon and identification of listeria monocytogenes determinants, including the peptidyl-prolyl isomerase PrsA2, that contribute to its hemolytic phenotype. *Journal of Bacteriology*, *191*, 3950–3964.

SUPPORTING INFORMATION

Additional supporting information can be found online in the Supporting Information section at the end of this article.

How to cite this article: Cahoon, L. A., Alejandro-Navarreto, X., Gururaja, A. N., Light, S. H., Alonzo, F., Anderson, W. F. & Freitag, N. E. (2022). *Listeria monocytogenes* two component system PieRS regulates secretion chaperones PrsA1 and PrsA2 and enhances bacterial translocation across the intestine. *Molecular Microbiology*, *118*, 278–293. https://doi.org/10.1111/mmi.14967